## Progress reports of individual researchers

**ASADA, Yasuo** **Energy**
Asymmetric Reduction of Phenyl-Ketones by a photosynthetic bacterium, *Rhodopseudomonas palustris*No.7

**ASAI, Tomohiko** **Nanomaterials and Nanodevices**
Control and Application of Self-organized Magnetized Plasmoid

**CHAEN, Shigeru and TOJO, Tadashi** **Nanomaterials and Nanodevices**
Single-Molecule Imaging of Bionanomachines

**FUJIWARA, Kyoko and NAGASE, Hiroki** **Medicine**
1. PI polyamide targeting MYC downstream genes for anti-neurobalstoma therapy
2. SAHA and PI polyamide conjugate for genome specific histone modification
3. Radiation induced photodynamic therapy

**FUKUDA, Noboru** **Medicine**
1. Drug discovery of PI polyamide targeting TGF-b1
2. Induction of human iPS cells with PI polyamide targeting human TGF-b1
3. Development of molecular imaging for primary aldosteronism

**HASHIBA, Hideomi** **Information Group ; Nanomaterials and Nanodevices**
Nano-sized structures for single-photon or single electron devices and applications for quantum information, energy areas

**HASHIMOTO, Takuya** **Energy**
Preparation of Materials for Intermediate Temperature Solid Oxide Fuel Cells with Nano-mixing Process

**IKAKE, Hiroki** **Supramolecules and Self-Assembly**
Development of Poly(lactic acid)s Films as biopolymer, and Applications to New Material Field

**INOUE, Shuichiro** **Information**
Development of Elemental Technologies for a Quantum Repeater

**ISHIDA, Hiroshi** **Quantum Theory and Computation**
Cluster Dynamical Mean-field Calculation of the Electronic Structure of the 2-Dimensional Hubbard Model Adsorbed on a Metal Substrate

**ITOH, Akiyoshi and TSUKAMOTO, Arata** **Information ; Supramolecules and Self-Assembly**
Ultra High Density Information Recording Materials on Self-assembled Nano-structured Substrates

**IWATA, Nobuyuki** **Nanomaterials and Nanodevices**
Pursuing the Limits of Nanomaterial-based Photonic and Quantum Technologies

**KOSHINAGA, Tsugumichi** **Medicine**
Potential of new therapeutic and diagnostic technology using PI polyamide and nanostructure in neuroblastoma

**KUWAMOTO, Takeshi** **Information**
Experimental Studies for Quantum Memory with Neutral Atoms

**MATSUMOTO, Yoshiaki and AOYAMA, Takahiko** **Medicine**
Pharmacokinetic/Pharmacodynamic Modeling of Tumor-localizing Photosensitizing Compounds

**MATSUSHITA, Sachiko** **Supramolecules and Self-Assembly ; Energy**
Self-assembly and Self-organization from the viewpoint of Device-fabrication Methods

**MOCHIZUKI, Shosuke** **Nanomaterials and Nanodevices**
UV-laser-light-induced photoluminescence spectral change of various metal oxides

**NAKAGAWA, Katsuji** **Information**
Thermally Assisted Magnetic Recording with Near-Field Plasmon Antenna

**NISHIMIYA, Nobuyuki** **Energy**
Composite Formation of Hydrogen Occlusion Alloys and Photo-Related Phenomena Thereof

**OHNUKI, Shinichiro** **Quantum Theory and Computation**
Design of Nanoscale Devices using Electromagnetic Simulation

**OTSUKI, Joe** **Supramolecules and Self-Assembly; Energy**
Self-Assembled Supramolecules and Their Applications to Energy, Medical, and Information Technologies

**SAKO, Tokuei** **Quantum Theory and Computation**
Origin of Hund's multiplicity rule in He-like atoms: Existence of conjugate Fermi hole in the lower spin state

**SUZUKI, Kaoru** **Nanomaterials and Nanodevices**
Synthesis of Nano-rod Devices with Wide Band Gap Semiconductor Effect

**TAKANO, Yoshiki** **Nanomaterials and Nanodevices**
Mechanism of Superconductivity in Layered Fe-based Superconductors and Search of New Superconducting Compounds

**TSUKAMOTO, Arata and ITOH, Akiyoshi** **Information ; Supramolecules and Self-Assembly**
Ultra Fast Information Recording and Ultra Fast Photo Magnetic Switching

**YAMASAKI, Tsuneki** **Quantum Theory and Computation**
Propagation Characteristics of Dielectric Waveguides with Arbitrary Inhomogeneous Media in the Middle Layer

# Asymmetric Reduction of Phenyl-Ketones by a photosynthetic bacterium, *Rhodopseudomonas palustris*No.7

**Yasuo ASADA , Ken-ich ITOH, Katsuhiro ISHIMI, Hideki KOHNO**
Energy

The intact cells of cyanobacteria, *Synechococcus* PCC6803 and PCC7942 were found to asymmetrically reduce phenyl-ketones and the related compounds including isoxasoles (Itoh, et al.).. However, the rate is low, and the responsible enzyme(s) is not known. We found the intact cells of alcohol-asimilating photosynthetic bacterium, *Rhodopseudomonas palustris* No.7 asymmetrically reduced isoxazole to its s-type alcohol in 95-96 % e.e.

In this symposium last year, we reported that three putative alcohol dehydrogenase (ADH) genes from PCC6803 and the ADH gene from *Rh.palustris* No.7 were transferred into a non alcohol-assimilating photosynthetic bacterium, *Rhodobacter sphaeroides* RV by conjugative system (Vasylieva et al., Appl. Biochem.& Biotechnol., **77-79**, pp.507-512, 1999) and that all the transconjugants have ADH activity for short chain alcohols.

Recently, we observed that the intact cells of wild strain *Rh.palustris* No.7, and transconjugants with （No.7 and cyanobacterial sll1825, slr0886 and slr0942 genes）assymetrically converted penta-fluoro-acephophenon to their s-form alcohols.

## Control and application of self-organized magnetized plasmoid

**Tomohiko ASAI**
Nanomaterials and Nanodevices

Self-organized magnetized plasmoid has attractive advantages for the variety of applications because of its wide range of plasma parameters and its ease of control. In this work, applications of the plasmoid for rapid thin-film deposition and EUV light source have been proposed and demonstrated. Also, several innovative applications of plasma formation technique have been proposed and initiated in this project.

### 1. Development of high-speed film deposition technique by magnetized coaxial plasma gun

MCPG has been applied for new alloy film deposition technique using a magnetized coaxial plasma gun (MCPG). This method enables application of high-melting-point metals (e.g., Ti, Zr …) which had been a limited method of ion beam assisted vacuum deposition etc. The optimization of gun design and the initial experiment with stainless steel electrode have been performed. In the experiments with horizontal plasmoid ejection into 500mm long drift tube, metallic thin-film was deposited on the vertically placed substrate. As a result of this preliminary test, electrode with composite material have been built and generation of alloy film will be started in the near future.
(Collaboration with Prof. K. Suzuki and Prof. N. Nishimiya)

### 2. High frequency repetitive operation (10kHz) and merging of Spheromak for VUV light source

An ionized plasmoid generated by MCPG tends to be relaxed into a force-free equilibrium called "spheromak" in a conductive metallic chamber which roles as a flux conserver. Counter injection of spheromaks into the flux conserver is followed by a magnetic reconnection event which heats the plasma itself by the dissipation of magnetic energy into plasma energy. This realizes a compact high-temperature plasma source which can be applied as a short wavelength light source. In this year, the dependency of emission and its profile on the geometry of poloidal and toroidal magnetic flux has been studied as an additional control method of emission profile using a compact coaxial plasma gun shown in Figure 1.

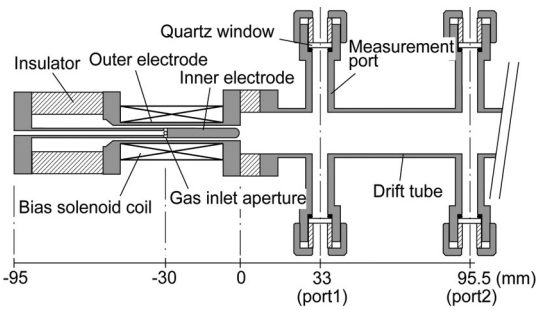


Figure 1. Schematic of developed compact magnetized coaxial plasma gun for EUV light source.

### 3. Electrodeless plasma source using rotating magnetic field

Steadily operated plasma source using rotating magnetic field (RMF) technique has been studied aiming to the applications for a light source and a plasma treatment method. The application of magnetic circuit on RMF antenna has been realized higher efficiency of plasma formation. Patent application has been prepared through NUBIC. (Collaboration with Dr. M. Inomoto, University of Tokyo)

### 4. Plasma treatment of CNT and CNT/polymer composite

An atmospheric-pressure plasma source with LF (~10kHz, 10kV) discharge for plasma treatment on CNT and CNT/polymer composite has been initiated to develop as collaboration with Dr. H. Ikake.

# Single-Molecule Imaging of Bionanomachines

**Shigeru CHAEN and Tadashi TOJO**
Nanomaterials and Nanodevices

In studies on bio-nanomachines, the conventional ensemble techniques have been used. However the ensemble of many bio-nanomachines does not represent the real view of the bio-molecule, because the individual reaction does not intrinsically synchronizes with each other. Studying single-molecule at a time is necessary for understanding the bio-nanomachine in action. Here we report studies on the biomolecular motor using the ordinary fluorescent imaging and the receptor protein on the biomembrane using the single-moecule fluorescent imaging technique.

## 1. Studies on the biomolecular motor using the ordinary fluorescent imaging technique.

In vitro motility assays using bipolar myosin thick filaments demonstrated that actin filaments were capable of moving in both directions along the myosin filament tracks. The movements, however, were slower in the direction leading away from the central bare zone than towards it. To understand the mechanism underlying these different direction-dependent motilities, we have examined the effects of temperature on the velocities of the bidirectional movements along reconstituted myosin filaments. The apparent activation energy of the movement away from the central bare zone was significantly higher (79 kJ/mol) than that of the movement toward the zone (44 kJ/mol). Given that the backward movement away from the central bare zone would cause the myosin heads to be constrained and the stiffness of the cross-bridges to increase, these results suggest that the elastic energy required for the cross-bridge transition is supplied by thermal fluctuations. (publication 2).

## 2. Studies on the receptor protein on the biomembrane using the single-moecule fluorescent imaging technique

Single molecule imaging technique has broken through the bottlenecking problem of optical resolution limit and provided a method to directly observe each single molecule by optical microscopy. Traditional epi-fluorescence microscopy can not identify faint fluorescence from a single molecule buried in enormous amount of background fluorescence. Evanescent field illumination method provides a device for drastically reducing background fluorescence and enables *in vitro* single molecule imaging of purified proteins. The method, however, has several problems to overcome in *in vivo* usage. Intense and heterogeneous distribution of autofluorescence in living cells or tissues is a deep-rooted obstacle to reduce background. Brownian motion of objective molecules bring about spaciotemporally ever-changing distribution of their fluorescence intensity. To surmount these difficulties, we have improved our microscopy system to accomplish high contrast imaging and investigated alternative fluorescent reagents instead of GFP. We have so far singled mPlum, a fluorescent protein, out for High S/N ratio and long lifetime of its chromophore. We intend to evaluate *in vivo* usage of mPlum. In practice, we conduct *in vivo* single molecule imaging of a fusion protein consisting of Plasma Membrane Targeting sequence (PMT) and mPlum expressed in living cells. PMT sequence makes it possible to place the fusion protein directly under plasma membrane.

# Applied chemical biology: strategy to cure cancer patients
## 1. PI polyamide targeting MYC downstream genes for anti-neurobalstoma therapy
## 2. SAHA and PI polyamide conjugate for genome specific histone modification
## 3. Radiation induced photodynamic therapy

**Kyoko FUJIWARA, Makoto KIMURA, Rajeeve MISHRA, Xiaofei WANG, Takayoshi WATANABE, Jun IGARASHI, Chen MING, Hiroki NAGASE**
Medicine

Our aim is development of nano technological approaches for clinical application. Under the close collaboration with Professor Joe Otsuki we conducted above three projects to generate new anticancer drugs or diagnostic reagents by using organic chemical synthesis techniques.

**1. PI polyamide targeting MYC downstream genes for anti-neurobalstoma therapy**

We developed a novel approach in cancer therapeutics using sequence specific DNA binding Pyrrole-imidazole (PI) polyamide, which designed to bind the E-box sequence of MYC downstream genes in a target specific manner, thereby down-regulating gene and protein expression of these genes. Furthermore it also suppresses MYC-dependent tumorgenesis in SCID mice by inhibiting proliferation and inducing apoptosis. Conclusively our findings suggest that E-box binding PI polyamide can be used in MYC-targeting therapies for cancer treatment.

**2. PI polyamide-SAHA conjugate for genome specific histone modification**

There is increasing evidence that histone modification is a crucial epigenetic modification of the mammalian genome, regulating not only transcription regulation but also many other cellular processes. Epigenetic changes are also associated with many diseases and environmental effects in humans. We tested whether newly developed PI polyamide and Suberoylanilide hydroxamic acid (SAHA) conjugates are able to induce histone acetylation at the target genomic region and the target gene expression. Presence of histone acetylation at target regions within p16 Cyclin-Dependent Kinase Inhibitor 2A (CDKN2A) and *LARP1* promoters was demonstrated after WGCWGGCW targeting PI polyamide-SAHA conjugate treatment. Although p16 tumor suppressor was not induced, the treatment induced LARP1 transcription and cell growth arrest in three different human cell types. Exogenous *LARP1* overexpression in the HeLa cell also induced similar cell-growth inhibition. The PI polyamide moiety can be an intriguing carrier of HDAC inhibitors or chromatin regulators to a specific DNA sequence and may modulate histone structure for a target gene expression.

**3. Radiation induced photodynamic therapy using iodinated photosensitizer**

Parametric monochromatic X-ray (PXR) is a new class of coherent X-ray, which is a tunable single wavelength and single phase X-ray. Since PXR is a single wavelength and single phase of soft-to-hard X-ray, it minimizes radiation exposure in the surrounding tissues and may have a potential to induce photoexcitation of radiosensitive molecules and establish a new PDT antitumor therapy targeting deep internal tumors and metastatic regions. PDT compounds conjugated with Iodine, which has a K-edge absorption of around 33KeV and generate singlet oxygen for the radiation induced photodynamic therapy. We have confirmed that compounds 531 and 717 showed cancer cell growth inhibition after irradiation.

# 1. Drug discovery of PI polyamide targeting TGF-b1
# 2. Induction of human iPS cells with PI polyamide targeting human TGF-b1
# 3. Development of molecular imaging for primary aldosteronism

**Noboru FUKUDA, Akifumi IGUCHI, Kousuke SAITO, Yukihiro IKEDA**
Collaboration: Frolida Univ. Dept. Pathology. K. Shinohara and N. Terada
Nihon Univ., Coll. Bioresource Sci., Y. Masuhiro, S. Hanazawa
Medicine

## 1. Drug discovery of PI polyamide targeting TGF- b1

1) Effects of PI polyamide targeting TGF- b1 on encapsulating peritoneal sclerosis (EPS)

Polyamide was ip injected once or 3 times in rat model of EPS. Polyamide significantly suppressed thickness of peritoneum. Polyamide significantly suppressed abundance of TGF-b1 and fibronectin mRNAs in injured peritoneum. Average of elasticity was significantly lower in Polyamide-treated rats than that in CHX-treated rats. Thus Polyamide is feasible for EPS.

2) Lead optimization of PI polyamides targeting human TGF-b1

We synthesized seven PI polyamides targeting human TGF-b1 on sis-elements of TGF-b1 promoter. We chose three lead optima such as GB1101, GB1105, GB1106 by inhibition of human TGF-b1 mRNA expression. We are examinig effects of these polyamides on expression of TGF-β1, fibronectin、collagen type IV, CTGF mRNA and EMT phenomena in human VSMC.

## 2. Induction of human iPS cells with PI polyamide targeting human TGF-b1

Certain mechanisms underlying the induction of iPS cells with Yamanaka 4 factors has been clarified as the Mesenchymal Epithelial Transformation(MET) phenomen at 2010. We started a collaborating project to induce human iPS cells by PI polyamide targeting human TGF-b1 with Florida University and Nihon Univ. Coll. Bioresource Sci.

## 3. Developemnt of the molecular imaging for aldosteronism with antisense PNA

We confirmed increases in expression of CYP11B2 mRNA in cultured Y1 cells with ACTH. We incuvated antisensei FITC-lebeled PNA targeting CYP11B2 in Y1 cells. We are checking timing of the fluorescence detecting.

# Nano-sized structures for single-photon or single electron devices and applications for quantum information, energy areas

**Hideomi HASHIBA**
Information; Nanomaterials and nanodevices

Appropriate nano-sized shaping of semiconductors shows quantum effects of electrons and photons, and forms quantum dots, photonic crystals, or single photon waveguides.
The aim of this work is development of a THz single photon detector with a quantum dot, $TiO_2$ photonic crystals for dye sensitized solar cells, and Si waveguide for quantum information on-chip devices. These devices will reveals deep understanding of physics such as photon-electron interactions, and open up wide applications to research or industrial area. The researches are closely collaborated with the *N*. research members for searching for applications of quantum information technologies and energy use.

## 1. Sensing individual terahertz photons

One of the promising ways to perform single-photon counting of terahertz radiation consists in sensitive probing of plasma excitation in the electron gas upon photon absorption. We demonstrate the ultimate sensor operating on this principle. It is assembled from a GaAs/AlGaAs quantum dot, electron reservoir and superconducting single-electron transistor. The quantum dot is isolated from the surrounding electron reservoir in such a way that when the excited plasma wave decays, an electron could tunnel off the dot to the reservoir. The resulting charge polarization of the dot is detected with the single-electron transistor. Such a system forms an easy-to-use sensor enabling single-photon counting in a very obscure wavelength region. The detector shows high noise equivalent power of ~$10^{-19}$ $WHz^{-1/2}$ （Paper. 1）.

## 2. Two dimansional titanium di-oxide photonic crystal for dye sensitized solar cells

Low dimension photonic crystals have drawn much attention as key-devices to on-chip optical systems, dye sensitized solar cells that are low cost, environmental friendly.
Our two dimensional titanium di-oxide photonic crystals are fabricated on a ITO wafer with a standard electron beam lithography. $TiO_2$ photonic crystals are periodic square air holes on a $TiO_2$ layer of 150 nm thick formed on a ITO conductive glass. The structure is designed for having photonic full band gap at wavelength of 630 nm to improve conversion efficiency of light to current in dye-sensitized photonic cell and has been reported (Paper. 2).

## 3. Development of Si waveguides as onchipon chip component for optical quantum cryptography comunications

Si waveguide is Silicon core of diameter of half wavelength of incoming photons, surrounded by highly refractive SiO2 or vacuum. Its characteristic of optical non-linearity of the semiconductor and single mode transmission, thus Si waveguides can be good candidate of photonic on chip component for optical quantum cryptography communications. We developed of Si waveguides with simple fabrication techniques.

# Preparation of Materials for Intermediate Temperature Solid Oxide Fuel Cells with Nano-mixing Process

**Takuya HASHIMOTO**
Energy

Solid oxide fuel cell (SOFC) attracts much interest as energy conversion device with high energy efficiency and low cost owing to no necessity of Pt catalyst in electrode. However, instability during long period and a few alternatives for materials due to too high operating temperatures are problems for application. Decreasing operating temperature as low as about 600 ºC would solve the problems. The purpose of this study is development of new electrolyte and electrode materials which are inevitable for low temperature operation of SOFC. In particular, using liquid phase process by which mixing with nano-scale is probable, challenged is preparation of high functional new materials whose preparation have been difficult or mechanical strength and density is low with conventional solid state reaction process.

In this year, following two themes have been investigated.

1. Preparation of new proton conductor, $Sr_{1-x}Ba_xZrO_3$ with liquid phase mixing method.
2. Preparation of new electrode material, $LaNi_{1-x}Fe_xO_3$

In this presentation, results of former theme are presented.

So far, electrode material for SOFC is oxide ion conductor such as yttria stabilized $ZrO_2$ (YSZ). It possesses high chemical stability and mechanical strength, however, high temperature as high as 900 ºC is necessary to obtain enough oxide ion conductivity. We regard that high temperature is inevitably required for conduction of large oxide ion and that proton conductor must be investigated and new one should be discovered for development of new electrolyte materials operated at low temperature.

$SrZrO_3$ and $BaZrO_3$ with distorted perovskite structure have attracted much interest as proton conducting oxides. It has been reported that oxide ion vacancy generated by partial $Y^{3+}$ substitution for $Zr^{4+}$ site plays the important role for proton conduction. However, three kinds of structural phase transition in $SrZrO_3$ are problems for application. In this study, we have succeeded in clarification of the phase transitions using high-temperature X-ray diffraction, differential scanning calorimetry and dilatometry. We have also prepared specimens with no first order structural phase transition from room temperature to 1200 ºC by partial substitution of Ba above 0.6. In addition, from comparison of specimens prepared by liquid phase mixing method and solid state reaction method, it has been revealed that liquid phase mixing method is superior for preparation of specimens with high density. This shows agreement with random and facet growth in the specimens of $Sr_{0.4}Ba_{0.6}ZrO_3$ prepared by solid state reaction method and liquid phase mixing one, respectively, as shown in Fig. 1.

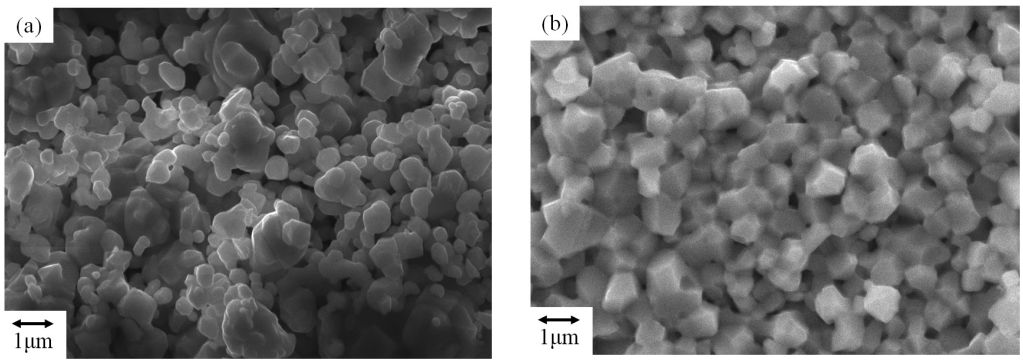


Fig. 1 SEM images of $Sr_{0.4}Ba_{0.6}ZrO_3$ ceramics prepared with (a) solid state reaction method and (b) liquid phase mixing method.

# Development of Poly(lactic acid)s Films as biopolymer, and Applications to New Material Field

**Hiroki IKAKE**
Supramolecules and Self-Assembly

In our group, the aim of development of poly(lactic acid) (PLA) films as biopolymer with the high thermal- and mechanical- resistance. And then, the improved PLA was submitted to new material field.

## 1. Development of Poly(lactic acid) Films with Exhibiting the Piezoelectricity

It is well known that poly(L-lactid) (PLLA) fibers exhibit the piezoelectricity, in which their piezoelectric constant increases with increasing degree of crystallinity and uniformity of the orientation of the crystallites. Recently, bending motion due to their piezoelectricity has been reported. The *zigzag* motion is closely related to the morphology of PLLA fibers. For this purpose, the irradiated magnetic field, and other process, under the electric field, have produced the high oriented PLLA films. In the present study, we successfully synthesized PLLA using condensation polymerization, and the crystallites of PLLA became the growth by the heat treatment.

## 2. Preparation of Poly(lactic acid)/Silica, and /Carbon Nanotube Hybrid Materials

In this work, the transparent hybrid materials were prepared with modified both chain ends of poly(D, L-lactic acid) (PDLLA) with silane-coupling agents and silica by the sol-gel process. It was clarified that the hybrid film having 10wt% $SiO_2$ is transparent, and the three-dimension network structure has been developed. Therefore, the thermal-resistance of the hybrids was improved at the rubbery plateau region. For next work, the aim of high mechanical-resistance, we prepare PLLA/Carbon Nanotube hybrid materials by the sol-gel process.

## 3. Preparation of Stereo-complex type Poly(lactic acid) Films

The study of the effect of cast-solvent on the morphology of the stereo-complex poly(lactic acid) (sc-PLA), consisting of poly(L-lactic acid) PLLA and poly(D-lactic acid) PDLA, is crucial for the sake to employ it as one of useful materials. In this study, it is clarified that the cast-film formed with 1,4-dioxane as a cast-solvent is opaque, but the film formed with chloroform is transparent. It is shown by small-angle X-ray scattering, differential scanning calorimetry, and wide-angle X-ray diffraction that, while the distribution of the crystal-domains of sc-PLA has remarkably depended on these cast-solvents, the degree of crystallization of sc-PLA as well as its crystal form was substantially independent of these cast-solvents.

# Development of elemental technologies for a quantum repeater

**Shuichiro INOUE**
Information

Quantum information and communication are the promising technologies that give us the solutions for the security and the communication capacity problems of the current information and communication technologies. The aim of our research is the practical implementation of the BBM92 quantum key distribution which allows us to communicate with the unconditional security. We are developing elemental technologies for a quantum repeater which is the key technology of the next-generation quantum key distribution system.

## 1. High rate distribution of entangled photon pairs at telecommunication wavelength

We demonstrated the distribution of a cross-polarization-entangled photon pair which is generated using a Type-II PPLN waveguide. To achieve a high-rate distribution of entangled photon pair, we used the high-speed and efficient single photon detector based on the sinusoidally gated InGaAs/InP avalanche photodiodes (SG-APDs). Figure 1 shows the experimental results of the polarization correlation tests when the average photon pair number per pulse was set to 0.01. The measured two photon interference visibility was 97 %. Moreover, the entanglement distribution rate exceeded 2.8 kilobit per second. To our knowledge, this value is the highest distribution rate in the entanglement distribution experiment at telecommunication wavelength to date.

## 2. Development of High Detection Efficiency Photon-Number-Resolving Detectors at 850 nm

Photon-number resolving detectors are indispensable requirements for many quantum information applications, such as quantum key distribution (QKD) and quantum optical gate. We have developed titanium-based transition edge sensors (Ti-TESs) to improve the response speed of the sensor. In order to achieve the almost 100 % detection efficiency (DE) at 850 nm wavelength, we fabricated Ti-TESs with the mult-layerd absorption structures, which consist of a 20-layer dielectric mirror and a 7-layer AR coating. The size and the thickness of the Ti film are 10 μm×10 μm and 22 nm, respectively. Figure 2 shows the pulse height spectrum from the Ti-TES in response to 844 nm (1.47 eV) photon pulses. We can discriminate each peak that corresponds to the number of absorbed photons in the TES. We have measured the DE at various different laser power levels. As a results, the DE at 844 nm was 98.4 %, which to our knowledge is the highest DE reported for an optical photon detector.

# Cluster Dynamical Mean-field Calculation of the Electronic Structure of the 2-Dimensional Hubbard Model adsorbed on a Metal Substrate

**Hiroshi ISHIDA**
Quantum Theory and Computation

Recently, heterostructures made by stacking ultrathin layers of strongly correlated materials have been a target of intense study. Due to low-dimensionality, charge transfers etc., the electron system at crystal interfaces exhibits properties absent in bulk systems, which can be utilized for new electronic devices. In this study, we investigate the electronic structure of strongly correlated interfaces by conducting many-body calculations within the dynamical mean-field theory (DMFT).

## 1. Electronic structure of strongly correlated atomic overlayer on a metal substrate

Previously, we studied the electronic structure of strongly correlated ultrathin films by taking account of interlayer electron correlations. However, in that work, electron correlations within the same atomic layer were ignored (publication 2). Thus, in the present study, we investigate the effects of intralayer electron correlations on the electronic structure of the strongly correlated atomic overlayer on a metal substrate.

The overlayer was modeled by a single-band Hubbard model on square lattice. To simulate a cuprate overlayer, we set t'= -0.3 t and U=9t, where t, t', and U denote the nearest-neighbor transfer integral, second nearest-neighbor transfer integral, and onsite Coulomb energy, respectively. The substrate was modeled by a semi-infinite non-interacting cubic lattice with band width W=12 t. The orbital mixing between the overlayer and substrate was expressed by a transfer integral between the atomic site in the overlayer and that in the outermost substrate layer, $t_z$. To treat short-range intralayer electron correlations, we performed a cluster DMFT calculation, where the overlayer was divided into a periodic array of 2x2-site clusters.

The electronic density of states (DOS) in the overlayer is shown for U=0 with $t_z$/ t=0.2, 04, and 0.8 (Fig.1 in the first page). The van Hove singularity in DOS characterizing the 2-dimensional square lattice disappears with increasing orbital hybridization between the overlayer and substrate. The electron occupation per spin is plotted as a function of electron chemical potential μ for t'= -0.3 t and U=9t (Fig.2 in the first page). When $t_z$=0, the system is purely 2-dimensional and becomes a Mott insulator in the energy gap where the occupation takes a constant value 0.5. The metal-insulator transition on the hole-dope side is of the second order, while that on the electron-dope side is of the first order, exhibiting hysteresis behaviors. In the case of $t_z$/ t= 0.8, the overlayer becomes metallic and $dn/d\mu > 0$ irrespective of the value of μ because the metal penetrates into the overlayer due to orbital hybridization. However, the phase transitions on the hole and electron doping sides persist, which indicates that the electronic structure of the overlayer is essentially close to that of the isolated layer. This is in contrast with the physical picture obtained with the single-site DMFT calculation where the overlayer exhibits Fermi-liquid properties when $t_z > 0$.

# Ultra High Density Information Recording Materials on Self Assembled Nano-structured Substrates

**Akiyoshi ITOH, Arata TSUKAMOTO**
Information Storage; Supramolecules and Self-Assembly

## 1. Resarch aim

In recent years, much attention has been focused on nano-structured magnetic media for achieving ultra high density recording. Combining self-assembly nano-structured substrates with defined magnetic properties provided by a magnetic film deposited onto the surface, enable a noble approach to create magnetic nanostructure arrays. We tried to prepare and utilize nano-structured substrates such as silica thin film having self-assembled nano-pores and self-assembled silica particle substrate.

Concrete plan was as followings.

1) Self assembled preparation of three dimensional close-packed nano structure arrays
2) Development of nano template substrate for preparing a nano structured metallic material
3) Application for ultra high density information recording material

## 2. Research plan /Advances and achievements in 2010

We focused onto preparation of a thin nano-porous silica film and application as etching musk of metallic film, and then examined 1. Enlargement of the areal size of single domain nano-pore array structure, 2. Thinning the silica layer with aligned nano pore array structure as 2 dimensional nano-pore allay structure, 3. Fabrication of a silica layer on metallic films.

2-1 Preparation of a thin nano-porous silica film and application as etching musk of metallic films

We have succeeded preliminarily to prepare thin silica layer on metallic films which have two dimensional closed packed nano-pores prepared by the polymer micelles technique.

1. By reducing the molecular weight, the average diameter of nano-pores was decreased from 8nm to 5nm. Furthermore, the areal size of single domain nano-pore array structure was enlarged up to around $1\mu m^2$ ($> 8.8 \times 10^5\, nm^2$) by reconsideration of fabrication process especially the sequence of compound molecules. See Fig. 1.
2. Nano-porous Silica layer was prepared by utilizing self-assembling phenomenon with main components of triblock copolymer(A), Tetra-Eth-Oxy-Silane (TEOS)(B), water with HCl(C) and Ethanol(D). Ethanol evaporates with drying process. By increase just the amount of Ethanol with keeping same ratio of other components A – C, prepared silica layer thickness was successfully reduced then achieved 2 dimensional nano-pore allay structure.
3. We have succeeded to prepare nano-porous silica film on metallic films such as Pt and Fe.

2-2 Nano structured template having a conjugate relation with nano-pore structure

As another type of nano structured template having a conjugate relation with nano-pore structure, nano convex pattern was prepared by using self-assembled spherical silica particles followed by inductively coupled plasma reactive ion etching.

# Pursuing the Limits of Nanomaterial-based Photonic and Quantum Technologies

**Nobuyuki IWATA**
Nanomaterials and Nanodevices

## 1. Selective growth of single-walled carbon nanotubes (SWNTs) with specific chirality

The triangle source and drain Au electrodes were evaporated on the $SiO_2$(300nm)/Si substrates using UV lithography and lift-off process. The area of electrodes and of between electrodes were left for 30 min in ozone atmosphere to be hydrophilic. The other area has surface property of bare $SiO_2$. The substrates were soaked for 10 min in ethanol where 0.01 wt% Mo acetate was dissolved, and were dipped at the speed of 600 μm/s. The dipped substrates were dried for 5 min at 500ºC. The catalyst of Co was deposited with the same process. The SWNTs were grown by an alcohol catalytic chemical vapor deposition (ACCVD) method. The used feeding source was ethanol. The growth was carried out at the pressure from 200 to 1000 Pa at 1050ºC after reduction under Ar and $H_2$ atmosphere. The free electron laser (FEL) of 800 nm was irradiated from start to end of growth process. The Raman spectra were detected with multiple excited laser of 441, 532, 632, and 785 nm. A scanning probe microscopy (SPM) checked the surface morphology.

The G-band and D-band peaks as well as radial breathing mode (RBM) in Raman spectra were observed at the only area between electrodes, the surface property of which was hydrophilic. The grown SWNTs were metallic and semiconducting materials, and included the chirality as many as approximately 50 without the FEL irradiation. Irradiating the 800 nm FEL reduced the number of possible chiralities down to 6 of (8,7), (10,6), (10,5), (12,2), (13,2), (13,0), (14,0), all of which show semiconducting property from the consideration of band structure. At the other area of substrate and electrodes, obvious G-band and the RBM peaks were not detected. In the SPM images, the random growth in direction of SWNTs were observed with approximately 1.5 nm in diameter and 1~2 μm in length. From those results, we successfully grew the selective SWNTs in position and chirality.

## 2. Fabrication of $REFeO_3/AFeO_3$ superlattices for realization of room temperature multiferroic phenomenon, where RE=Bi, La, A=Ca, Sr

The films and superlattices of $CaFeO_X$ (CFO), $SrFeO_X$ (SFO), $LaFeO_3$ (LFO), $BiFeO_X$ (BFO) were deposited on $SrTiO_3$(STO)(100) substrates by pulsed laser deposition (PLD) method with monitoring reflection high energy electron diffraction (RHEED) oscillation. The typical x-ray diffraction (XRD) and reciprocal space mapping around STO(103) and (113) were done. The SPM measurement showed the surface morphology.

The single layer of $CFO_{2.5}$, $SFO_{2.7}$, $LFO_3$, and four phases at least BFO were obtained. Using the highly dense, more than 90%, targets, the droplets were removed in all single layer films. In CFO/LFO superlattice, the satellite peaks were observed in the RSM, and the surface showed the step-terrace structure. Expected superlattice structure was [7units CFO / 7units LFO]×14. In CFO/BFO and SFO/BFO superlattice, the satellite peaks were also observed. From the results of low angle x-ray reflection from the surface, superlattice structures were [CFO(1.16nm) / BFO(1.30nm)]×14 and [SFO(1.36nm) / BFO(1.00nm)]×14. Those results were not exactly the films we tried to prepare, because the target surface changed and then growth rate was decreasing with continuing the deposition. The reason why we did not obtain the perfect and sharp satellite peaks in the RSM was same. There could be slight difference in thickness at each block in the superlattices. We have to find the right deposition condition, especially ablated laser energy. However, the presence of satellite peaks in superlattices indicates the not perfect but ordinary interface exists. Therefore polar / non-polar interface is expected.

# Potential of new therapeutic and diagnostic technology using PI polyamide and nanostructure in neuroblastoma

**Tsugumichi KOSHINAGA**
Medicine

Neuroblastoma (NB) is an embryonic tumor of neuroectodermal cells derived from neural crest. NB is the most common extracranial pediatric solid tumor and is caused around 15% of all pediatric oncology death. It has been strongly expected to develop new diagnostic maker and new therapy in NB. NB showing *MYCN* amplified usually have poor outcome and down regulation of *MYCN* expression causes down-regulated proliferation and differentiation in NB. PI polyamide can recognized specific DNA sequence and bind to it. When PI polyamide designed to target transcription factor binding site, it can inhibit binding of transcription factor to binding site and down-regulate a target gene expression. Here, we examine whether PI polyamide can show an antitumor effect. Moreover, this experiment could provide us basic data needed for development of new therapeutic and/or diagnostic agents by using PI polyamide combined with nanostructure.

## 1. *In vitro* experiments

We designed PI polyamide targeting SP1 and E2F binding site, which are located on promoter region of *MYCN* gene. NB cell lines, such as CHP134 cells were cultured with those PI polyamides, which are mixture of PI polyamides targeting SP1 and E2F binding site for 72 hours. NB cell lines showed reduced proliferation rate (a) and of MYCN expression level, compared with NB cell lines cultured without PI polyamides. Also NB cell lines treated with the PI polyamide presented apoptosis.

## 2. *In vivo* experiments

We made xenograft by injecting nudemice subcutaneously with NB cell lines, such as CHP134 cells. Then administration of PI polyamides into tumor carvities reduced growth rate of xenograft, compared with control polyamide (mismatch PI polyamide), which can not bind to SP1 and E2F binding site.

We confirmed that the PI polyamides, which are mixture of the PI polyamides targeting SP1 and for E2F binding sites have the antitumor effect. Accordingly, those PI polyamides and its modified form with new nanostructures could be one of new therapeutic agents and/or diagnostic agents.

# Experimental Studies for Quantum Memory using Neutral Atoms

**Takeshi KUWAMOTO**
Information

## 1. Our purpose in the project

Purpose of our study in this project is the experimental study for realizing the quantum memory using neutral atoms. The quantum memory is a key element in the quantum communication and computing.

## 2. Progresses and Results in 2010

We performed following studies this year.

(1) Measurement of the two-photon interference of orthogonally polarized photon pair with the 795-nm wavelength.

In last year, we succeeded to generate the orthogonally polarized photon pairs resonant with a transition in rubidium atom. However, we could not observe the two-photon interference, which ensures the quantum-mechanical nature of the generated photon pair. In this year, we performed following developments and studies as the countermeasure.

1. Reinforcement of the output power of 397.5-nm-wavelength light beam used for generating the orthogonally polarized photon pairs.
2. Exchanges for appropriate optics possessing no polarization dependence.
3. Production of new coincidence detectors.
4. Introduction of a crystal (5-mm KPT) used for compensating the birefringence effect in the crystal, which is used for generating the orthogonally polarized photon pairs.

We successfully measured quantum-mechanically the two-photon interference of the generated orthogonally polarized photon pairs. The obtained visibility was 83%.

(2) Suppression of the relative frequency fluctuations between two lasers used for the light storage experiments.

We have succeeded the storage of coherent light into rubidium atoms. However, the storage time was as short as 50 ms, which was a tenth of previous studies. We attributed this short storage time to the fluctuation of relative frequency between two lasers used in the experiments. We controlled the relative frequency of lasers using the optical phase lock loop (OPLL) circuit. As a result, the fluctuation was reduced from 2 MHz to 400 Hz, corresponding to a factor of 5000 improvement.

# Pharmacokinetic/Pharmacodynamic Modeling of Tumor-localizing Photosensitizing Compounds

**Takahiko AOYAMA, Yoshiaki MATSUMOTO**
Medicine

To describe the relationships between percent cures following photodynamic therapy, light dose, and plasma photosensitizing compound concentration, we defined the pharmacokinetic/pharmacodynamic model of talaporfin as a model drug.

## 1. Pharmacokinetic/pharmacodynamic modeling of Talaporfin in mice

Model-based drug development is characterized as the development and application of pharmacostatistical models of drug efficacy and safety from preclinical and clinical data to improve drug development knowledge management and decision making. Pharmacokinetic/pharmacodynamic modeling and simulation also enable the prediction of the effects of a medicine in various situations in clinical practice. The aims of this study were to define the pharmacokinetic/pharmacodynamic model of talapolfin as a model drug of tumor-localizint photosensitizing compounds and predict the response of photodynamic therapy in various dosage regimens. The plasma talaporfin concentration, percent cures following photodynamic therapy and light dose reported by Ferrario *et al*. were used as the source of pharmacokinetic/pharmacodynamic modeling data. The pharmacokinetics for talaporfin in mice was described by two-compartment model with first-order elimination. The relationships between the percent cures, light dose and plasma talaporfin concentration were described by Emax model (Fig. 1). Simulated curvilinear surface between percent cures, light dose, and plasma talaporfin concentration was well fitted the observed value (Fig. 2).

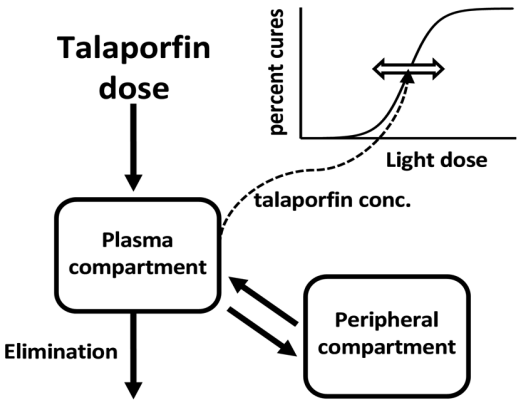


Fig. 1

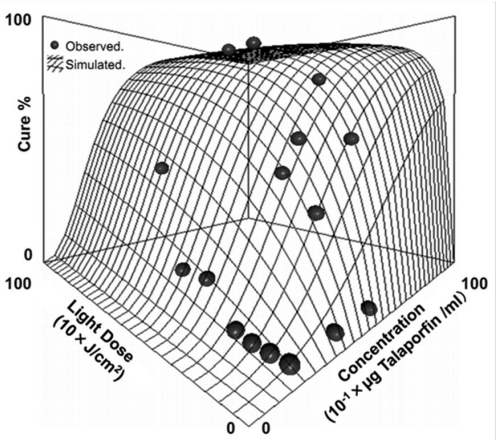


Fig. 2

## Self-assembly and Self-organization from the viewpoint of Device-fabrication Methods

**Sachiko MATSUSHITA**
Supramolecules and Self-Assembly; Energy

Three subjects related with self-assembly and self-organization were studied with perspective of the developments of unexplored scientific fields and new technology: 1) Dye-sensitized photonic crystal electrodes, 2) Fabrication of optical and diagnostic devices via self-assembly, and 3) Elucidation of mechanism of spontaneous tension change at oil/water interface.

### 1. Dye-sensitized photonic crystal electrodes

Recently, the combination of dye-sensitized solar cells and photonic crystals is actively studied. We had reported the improvement of the photoelectric conversion efficiency of dye-sensitized solar cells combined with a self-assembled-type photonic crystal, i.e., $TiO_2$ inverse opal. However, whether these results were caused by the photonic crystal effect or the nano/mesoscopic effect was unclear. The position of the photonic crystal band depends on the structural periodicity. Here, we prepared three kinds of $TiO_2$ inverse opals using different-size polystyrene particles (202 nm, 356 nm, 457 nm) and measured the electrochemical characteristics of the dye-sensitized inverse-opal electrodes. Figure 1 shows the electrochemical impedance of the prepared electrodes. The large diffusion resistance of the electrolyte suggests that the improvement of the photoelectric conversion efficiency was not caused by nano/mesoscopic effect because nano/mesoscopic effect should be appeared as small diffusion resistance. This research is a collaboration work with Prof. Hashimoto, College of Humanities and Sciences (one journal paper, *submitted*). This research was also awarded a poster prize.

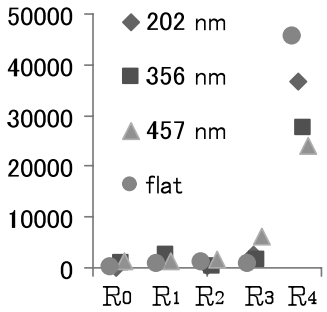


**Figure 1**. Pore-size dependence of electrochemical impedance of dye-sensitized $TiO_2$ inverse opals electrodes. $R_0$: Resistance of substrate, $R_1$: Resistance of substrate/$TiO_2$ interface, $R_2$: Contact resistance between $TiO_2$ particles, $R_3$: Pt/electrolyte interface and Electrolyte/dye/$TiO_2$ interface, $R_4$: diffusion of the electrolyte.

### 2. Fabrication of optical and diagnostic devices via self-assembly

Recently, the application of a self-assembled spherical-particle structure to hydrogels is actively studied. The application is mainly as sensors, for example, as a glucose sensor and temperature sensor. In this research, with the viewpoints of the applications as a cell culture substratum, a micro-pocket gel array was prepared by templating of a two-dimensional self-assembled structure composed of cell size particles. This work is a part of collaboration with Prof. Kano, College of bioresource science.

### 3. Elucidation of mechanism of spontaneous tension change at oil/water interface

The spontaneous oil movement in the water containing surfactants has been actively studied since Dupeyrat found this phenomenon in 1978. However, the perfect understanding of the spontaneous movement is still not achieved, resulting in less report of the concrete engineering applications. Recently, we focused on gels generated at the oil/water interface during the spontaneous movement. To control the gel generation, salt addition in the water phase was examined. The period and amplitude of the spontaneous movement were dynamically changed by salt concentrations.

## UV-laser-light-induced photoluminescence spectral change of various metal oxides

**S. MOCHIZUKI, K. YOSHIDA T. SAITO, F. MIZUTANI**
Nanomaterials and nanodevices

Mochizuki, Yoshida and Saito measured the photoluminescence spectra of bulk single crystal and nanocrystals of various metal oxides ($BaTiO_3$, $SrTiO_3$, $TiO_2$, ZnO, and etc) at different temperatures. We have found clear reversible spectral change in the photoluminescence spectra of the $SrTiO_3$ and $BaTiO_3$ specimens at room temperature by replacing the specimen atmosphere ($O_2$ gas by vacuum, $CO_2$ gas by vacuum) under CW 325 nm laser light irradiation. Especially, by irradiating at room temperature with the laser light in $CO_2$ gas atmosphere, the photoluminescence intensity of $BaTiO_3$ and $SrTiO_3$ nanocrystals with an average particle size of several ten nm is enhanced by more than ten times. By irradiating the same laser light at room temperature in a vacuum, the original weak luminescence state reappears. After removing the laser light irradiation, each photoluminescence property persists for a long time at room temperature under room light, regardless of any changes of atmosphere. On the other hand, $BaTiO_3$ bulk single crystal and $SrTiO_3$ one showed weak luminescence and little photo-induced changes. The observed reversible photo-induced phenomena in $CO_2$ atmosphere suggest that $BaTiO_3$ is active for photo-catalytic reduction of $CO_2$ at room temperature. The results are discussed also in the light of both the exciton theory and the defect chemistry.

Mizutani designed and made an evaluation device for photocatalyst and measured the photocatalyst power of various metal oxides..

# Thermally Assisted Magnetic Recording with Near-Field Plasmon Antenna

**Katsuji NAKAGAWA**
Information

Thermally assisted magnetic recording (TAMR) which is a next generation magnetic recording with ultra high recording density is investigated from viewpoints of a plasmon antenna and optical near-field by experiments and simulations in order to overcome physical limitation of recording density of current magnetic recording. Furthermore, a future magnetic memory applied with a photo-induced ultra-high speed magnetization phenomenon is also researched in close collaboration with Professor Itoh and Assistant Professor Tsukamoto. Analysis of surface plasmon is worked with Associate Professor Ohnuki who belongs to a quantum theory and calculation Group.

## 1. Thermally assisted magnetic recording with optical near-field

Issue of TAMR which is required for heating only nanometer-sized recording area is that influences of the distance from antenna to medium at heating and the plasmon antenna shape on recorded mark shapes are not clear. We proposed a new antenna configuration, which was available to confirm a plasmon antenna shape against magnetic domains recorded and to control antenna distance from medium at recording. We also constructed a fabrication process of the configuration, which was surface plasmon antennas with one hundred nanometer sized fabricated on a surface of a high recording density medium with high thermal stability, by lift-off method using e-beam lithography.

## 2. Surface plasmon antenna design

A heating on only tiny area, whose diameter is less than order of incident light wavelength, is required for TAMR. A surface plasmon antenna is designed by Finite-Difference Time-Domain (FDTD) simulation analysis to realize it (collaborated partially with Associate Professor Ohunuki). We have already reported that isolated fine-grain media was available to obtain high electric intensity. Further design of high efficiency plasmon antenna independent from medium structure which can obtain high intensity even continuous medium is enlarged the margin of medium selection. We realized increase of the antenna apex intensity and decrease of the antenna rears intensity at same time on the continuous medium by design of a tilt angle between antenna and medium.

## 3. Photo-induced ultra high magnetization recording

To increase recording density of novel magnetic recording system using a photo-induced ultra high magnetization phenomenon, we worked with Associate Professor Ohnuki in generation and concentration method of circularly polarized light on recording medium locally with optical near-field by a plasmon aperture. A cross aperture with four-fold symmetry can create circularly polarized light locally at the center of the aperture. We also show a propagation of circularly polarized light in the medium with an isolated fine-grain arranged rectangularly. In addition, we proposed a four-leaf shaped aperture modified the normal cross aperture, and demonstrated the improved the quality. The four-leaf aperture is available to confirm circularly polarized light with high intensity only at center fine-grain we will record, as a consequence of enlargement of intensity difference between center recoding grain and surrounding grains (Figure in first page, paper, patent, and Presentation). We investigated relative position margin between the aperture and the recording grain.

An analysis method of a transient response phenomenon of surface plasmon generation by simulation was investigated in collaboration with Associate Professor Ohnuki, and We developed into the electromagnetic transient analysis method which could apply nano-sized dispersion material and ensure accuracy of the calculation. It makes assumption of plasma frequency and transient analysis of arbitrary three-dimensional objects possible (Presentation).

# Composite Formation of Hydrogen Occlusion Alloys and Photo-Related Phenomena Thereof

**Nobuyuki NISHIMIYA**
Energy

## 1. Photo-Stimulated Hydrogen Desorption from Hydrogen Occluding Alloys

Complex hydride $LiBH_4$ desorbed hydrogen at room temperature as detected by mass spectrometry when irradiated by ultra violet (UV) light (g line) in the presence of both a photocatalyst $WO_3$ and a cocatalyst CuO, and did not when irradiated in the sole presence of either $WO_3$ or CuO. Hydrogen desorbing reactions without heating were unexpected and had not yet been reported.

On heating, pristine $LiBH_4$ desorbed hydrogen at 150℃ and 350℃, and these temperatures were lowered to 100℃ and 280℃ when the hydride was heated after UV irradiation in the presence of both the photocatalyst $WO_3$ and the cocatalyst CuO, as tabulated in Table 1. This means that UV irradiation can be employed to lower the hydrogen desorption temperature on heating, and that reinvestigation on many hydrogen occluding alloys with high hydrogen contents is necessary even if the hydrogen desorption temperatures are higher than practical ones (near 100℃).

Table 1 Characteristics of hydrogen desorption from $LiBH_4$

| | Heating in vacuo | Heating after UV irradiation | UV irradiation |
|---|---|---|---|
| $LiBH_4$ | Desorb at 150℃, 350℃ | Desorb at 150℃, 350℃ | None |
| CuO+$LiBH_4$(1:10) | Desorb at 80℃, 220℃ | Desorb at 280℃ | None |
| $WO_3$+$LiBH_4$(1:10) | Desorb at 150℃, 350℃ | Desorb at 100℃, 280℃ | None |
| $WO_3$+CuO+$LiBH_4$(1:1:5) | Desorb at 100℃, 280℃ | Desorb at 100℃, 280℃ | Desorb |
| $WO_3$+CuO+$LiBH_4$(1:1:10) | Desorb at 100℃, 280℃ | Desorb at 100℃, 280℃ | Desorb |
| $WO_3$+CuO+$LiBH_4$(1:1:16) | Desorb at 100℃, 280℃ | Desorb at 100℃, 280℃ | Desorb |

On heating after UV irradiation, hydrogen was released at 100℃ and 280℃ in the presence of $WO_3$ only with the cocatalyst CuO absent. On the other hand, the temperatures stayed at 150℃ and 350℃ without UV irradiation in the presence of $WO_3$ only. It is likely that the photocatalyst $WO_3$ destabilized hydrogen in the solid phase through irradiation to lower the desorption temperature. The cocatalyst CuO would catalyze the desorbing process, presumably recombination of hydrogen atoms. The desorbing temperatures were actually lowered to 80℃ and 220℃ when $LiBH_4$ was heated with CuO.

## 2. Recovery of Bio-Hydrogen Using Composite Hydrogen Occluding Alloys (Collaboration of Drs. Nishimiya and Asada)

Zirconium-based alloys, which were able to absorb low pressures of hydrogen, were encapsulated by dimethoxydimethyl silane-derived gel to be resistant to steam, oxygen and so on coexisting with fermented hydrogen. Microorganisms such as anabaena and spirulina were comparatively cultivated at 30℃ for several days under stressed conditions. About 6 mL of hydrogen was recovered from a 13.1 mL vial in an optimum run, which was 6 times as much as the case without any hydrogen occluding alloys. Since gaseous hydrogen in the absence of alloys was more than that in the presence of alloys, the alloys would occlude gaseous hydrogen to shift the hydrogen producing reaction of the microorganisms to the productive side.

# Design of Nanoscale Devices using Electromagnetic Simulation

**Shinichiro OHNUKI**
Quantum Theory and Computation

## Abstract

Fast and reliable electromagnetic simulation is performed for nanoscale objects which are relatively small in comparison with the wavelength of incident light. This work aims at designing novel nanoscale devices, such as nanoscale antennas to produce localized circular polarized light or plasmonic waveguides, and searching for application to information technology through the collaboration with researchers of the *N*. research project.

## 1. Design of Nanoscale Antennas for All Optical Magnetic Recording

For ultra-high speed recording, all optical magnetic recording with circularly polarized light has attracted attention. In this technology, recording is performed using left-handed and right-handed circularly polarized light. We study characteristics of a nanoscale dipole antenna and an asymmetric cross antenna is proposed to generate left-handed and right-handed localized circularly polarization from linearly polarized incident light. Figure 1 shows an asymmetric cross antenna constituted by two dipole antennas with common gap. Antenna lengths are selected to obtain 90° phase shift. Figure 2 shows the polarization characteristic for the incident direction 58° and 122°. Right-handed and left-handed circularly polarizations are generated at the center of antenna gap.

## 2. Analysis of Surface Plasmon by Complex Frequency Domain Integral Solvers

Recently, dynamics of specific plasmon modes has been intensively studied in terms of femtosecond techniques. We apply a boundary integral equation method together with the numerical inversion of Laplace transform to analyze specific plasmon modes. Our method is error controllable, stable for treating dispersive media, and suitable for parallel computing.

We also investigate surface modeling of nanoscale objects which are described by patches. The number of curvilinear patches is almost a half of that of triangular patches for smooth surface under the same computational accuracy.

## 3. High-Speed Analysis of Electromagnetic Problems Using Latest Parallel Processors

Fast and large scale computations are challenging problems in computational electromagnetics. We examine the potential of hardware acceleration for electromagnetic simulations using ultra high-speed processors with latest parallel technologies, such as a Cell Broadband Engine (Cell/B.E.) processor and a Graphics Processing Unit (GPU). Electromagnetic simulations using the method of moments (MoM) with an iterative solver can be accelerated by Cell/B.E. Large problems over 10,000x10,000 matrix can be treated by our proposed technique. The maximum speedup rate compared with a conventional CPU becomes 27 times faster. We also study ADI (Alternating-Direction Implicit) FDTD method which is known as one of the implicit methods. This FDTD method is suitable for investigating nanoscale problems, since the CFL condition can be avoided. Using GPU (Tesla C1060) and the CUBLAS library, the speedup rate becomes 25 times faster.

# Self-Assembled Supramolecules and Their Applications to Energy, Medical, and Information Technologies

**Joe OTSUKI**
Supramolecular and Self-Assembly; Energy

Self-assembly of appropriately designed molecules will afford a bottom-up method for producing nanostructures. This work aims at developing new molecular self-assembling systems, revealing self-assembled structures and dynamic behaviors at the molecular level, and searching for applications of self-assembly to energy, medical, and information technologies through the collaboration with researchers of the *N*. research project.

## 1. Structures and dynamic behaviors of molecular self-assemblies at the molecular level

Self-assembly of new double-decker complexes, in which two disk-like moieties, such as porphyrin and phthalocyanine, sandwich a metal ion, have been investigated. We have succeeded in capturing images by means of scanning tunneling microscopy that show the orientation changes over time, which afforded the first solid demonstration of the rotation libration of a double-decker complex (publication 1, Figure).

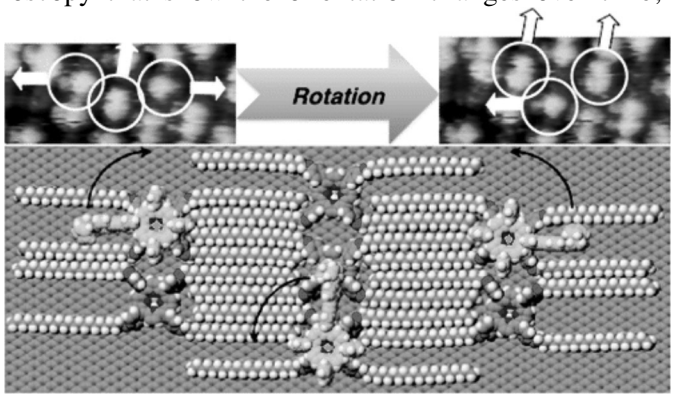


We have also reported systems in which self-assembly with a porphyrin molecule can be controlled by light irradiation by using newly synthesized molecules that change their shape on irradiation (publication 2).

## 2. Light-driven hydrogen evolution from water with self-assembled complexes

New iridium complexes have been prepared that have an additional coordination site. Upon mixing of one of these complexes and cobalt ion, the complex coordinates to the cobalt ion to form a supramolecular complex that contains both iridium and cobalt centers. It was expected that an electron transfer process occurs efficiently through the bonding between the iridium center, the photosensitizing site, and the cobalt center, the catalytic site. Some of them showed increased efficiencies in photodriven hydrogen evolution as compared to a case in which an iridium complex and a cobalt complex are not bound together (publication 3). Furthermore, we found that hydrogen evolving systems involving ruthenium complexes that recorded high turnover numbers without a catalyst.

## 3. Preparation of compounds for the X-ray based photodynamic therapy

Photodynamic therapy (PDT) is one of cancer treatment methods that destroys cancer cells by singlet oxygen produced by excited dyes accumulated in the cancerous region and formed under laser irradiation. The problem in this method is that visible-light laser used in the treatment cannot penetrate into the body more than 1 cm depth. In our attempt to combine X-ray irradiation, which penetrates well into the body, and the PDT, we have prepared porphyrin derivatives, effective in PDT, carrying iodine atoms, which absorb X-ray radiation (patent application 1). We have obtained some positive results in X-ray irradiation experiments at the cultured cell level. This is also scientifically very interesting because the unexplored physics must be involved in the energy transfer processes from the X-ray induced inner electron excitation to valence electron excitation.

# Origin of Hund's multiplicity rule in He-like atoms: Existence of conjugate Fermi hole in the lower spin state

**Tokuei SAKO**
Quantum Theory and Computation

Electron is the smallest magnetic unit in nature and has potential to become the smallest memory device with its spin degrees of freedom controlled properly. In the present study we focused on the so-called first Hund rule accounting for the relation between the total electron spin and the energy-level ordering in atoms, and clarified the origin of this rule operating in the simplest multi-electron atom He and He-like atomic ions.

Hund's rules consist of three rules that predict the ordering of the energy levels possessing different spin and orbital angular momentum quantum numbers. These three rules, particularly the first one concerning the spin multiplicity, proved to be almost universally valid not only for atomic systems, but also molecules and 'artificial atoms'. Concerning the origin of this first rule, a traditional interpretation given by Slater has been often quoted, which says that a higher spin state has a smaller electron repulsion energy. However, actual quantum chemical computations for singly-excited states of the helium atom, performed initially by Davidson and later many others, have showed that the triplet state with the higher spin multiplicity has a larger electron repulsion energy than does the corresponding singlet state possessing the lower spin. This indicates that the reason for a lower energy of the triplet state relative to the corresponding singlet cannot be due to a decrease in the electron repulsion potential, but must be ascribed to a more compact electron density distribution of the triplet state, which then results in a much larger energy decrease due to the nuclear attraction potential.

Nonetheless, there still exists an ambiguity concerning the reason why the triplet state has a more compact electron-density distribution than the corresponding singlet state. It was argued by Boyd that the Fermi hole induces a larger repulsion between electrons with parallel spins, which results in a larger average inter-electron angle of the triplet electrons than for the singlet electrons, thus allowing the triplet electrons to be closer to the nucleus thanks to the 'less screening' of the nuclear charge. On the other hand, very recently it has been shown by Moiseyev *et al*. that angular electron correlation is not important in the singly-excited states of helium in order to yield its energy levels accurately, although the triplet electrons may require to be angularly correlated to some extent in order to have a larger inter-electron angle. In our previous study [Paper 1], the origin of the Hund's multiplicity rule in two-electron artificial atoms was studied and the mechanism for the more compact electron density distribution in the triplet states was clarified by examining the nodal pattern of the wave functions in the internal space. Motivated by this earlier analysis the present study examines the internal wave functions of He in order to provide a deeper understanding into the workings of the first Hund's rule.

The internal part of the full configuration interaction wave functions for low-lying singlet-triplet pairs of states has been extracted and visualized in the three-dimensional internal space $(r_1, r_2, \phi_-)$. The electron-electron repulsion potential has been also visualized in the internal space. It manifests itself by three striking poles, penetrating exactly into the spatial region defined by the Fermi hole. Because of the existence of these strong potential poles in the vicinity of the Fermi hole, a major part of the singlet probability has to escape from this region. In contrast, the corresponding triplet wave function is less affected by these poles thanks to the presence of the Fermi hole. The evading singlet probability was shown to migrate far away from the original region close to the origin to the region where either $r_1$ or $r_2$ are large. This results in a more diffuse electron density distribution of the singlet state than the corresponding triplet state. The mechanism of the evolution of the singlet probability towards the large $r_i$ ($i$ = 1, 2) region in the presence of the electron repulsion potential has been rationalized on the basis of a new concept of the so-called *conjugate Fermi hole* [Paper 2].

# Synthesis of Nano-rod Devices with Wide Band Gap Semiconductor Effect

**Kaoru SUZUKI**
Nanomaterials and Nanodevices

My research aims at fabrication of nano-materials and nano-devices for high functional applications such as nano-tube sensor, nano-rod transistor and wide band gap semiconductor nano-film for water-splitting by using fundamental techniques of nano-process and fabrication of nano-materials. Using the achievement of the investigation, progress of energy conversion system, information technology and biotechnology can be expected.

## 1. Metal encapsulated carbon nanotube for magnetic force microscope probes

We have synthesized directly ferromagnetic metal (Ni, Fe, and Co) encapsulated carbon nanotubes (CNTs) for probe of magnetic force microscope on a mesh grid for viewing transmission electron microscope (TEM) by pyrolysis of ethanol solution. These metals inside CNTs identified Ni, Fe, and Co with energy dispersive X-ray (EDX) spectrum analysis. The diameter and length of the metal core is in the range of 10 – 80 nm and 100 – 800 nm with varying heating period and temperature, respectively. The walls consist of cylindrical graphene sheets with 3 -50 layer. The diameter of metal core possesses inclinable to enlarge at other temperature between 1013K and 1123K.

## 2. Synthesize of Photocatalytic SrxLa1-xTiO3 Film for Hydrogen Generation with Visible Area in Solar Light Excitation by Pulsed Laser Deposition

La doped TiO2 have attracted great interest for photocatalytic properties, which can be used visible area in solar light although only TiO2 limiting with ultra violet area. However, these reports were almost powdered La2Ti2O7. To circumvent this problem, we have attempted to synthesized La doped TiO2 thin film on quartz substrate by pulsed laser deposition using non-sintered target. In addition we have tried to Sr doped as imparity for improvement only hydrogen generation. These films were composed of several molar ratios. We have successfully crystallized perovskite structure films which were La doped TiO2 thin film of La2Ti2O7, Sr doped TiO2 thin film of SrTiO3 and both impurity doped thin film of SrxLa1-xTiO3 (x=0.1~0.9). The best of hydrogen generation efficiency was 16μℓ/hcm2 by Sr0.7La0.3TiO3 to SrTiO3, and furthermore, the band gap of Sr0.3La0.3TiO3 was 3.2 eV which showed the same tendency. As a result, the molar ratio of Sr0.7La0.3TiO3 thin film confirmed suitable to hydrogen generation.

## 3. Synthesis of (SrLaF)FeAs superconducting thin films by the photo excited pulsed laser deposition

The synthesis of the high $T_c$ superconducting thin films is very important for the electronic device use. Among Fe-based superconductors, a Co-doped $SrFe_2As_2$ epitaxial film is reported to become a superconductor with $T_c$ of 20 K. However, in order to obtain superconducting films by pulsed laser deposition (PLD), there are some problems such as expensive substrates and high quality target materials. The photo excited PLD (PE-PLD) is considered to have advantages for the synthesis of high quality epitaxial thin films. (SrLaF)FeAs is isostructural to (LaO)FeP and $(Sr_{0.6}La_{0.4}F)FeAs$ becomes superconducting below $T_c$ of 26.3 K. In this study, we have tried to prepare superconducting (SrLaF)FeAs thin films by PE-PLD, and investigated the relation between the wavelength of the photo excitation sources and the crystallization of films. They are deposited on MgO (001) substrates by PLD using a Nd:YAG laser (wavelength: 532 nm, fluence: 1.5 J/cm$^2$) with the photo excitation. The photo excitation sources are IR (from 0.5 to 2.5 μm), Xe (from 0.2 to 1.1 μm) and LED (peak: 400 nm, width: ± 20 nm). While X-ray diffraction patterns of (SrLaF)FeAs thin films excited by IR or normal PLD show only impurity phases, those excited by Xe or LED show some oriented peaks of (SrLaF)FeAs. This result indicates that the excitation by ultra violet rays increases a reaction ability and has an effective role of the growth of the superconducting epitaxial films.

# Mechanism of Superconductivity in Layered Fe-based Superconductors and Search of New Superconducting Compounds

**Yoshiki TAKANO**
Nanomaterials and Nanodevices

## 1. Introduction

Since $LaO_{1-x}F_xFeAs$ was discovered to be a superconductor with the superconducting transition temperature $T_c$ of 26 K in 2008, many superconductors which have Fe square lattices have been found. They are called Fe-based superconductors and have attracted much attention of many researchers.

We have focused our attention on SrFFeAs which crystal structure is as same as that of LaOFeAs (1111-type structure) and $Li_xFeAs$ which crystal structure is simpler than that of 1111-type structure (111-type structure). When a part of Sr site is substituted by rare earth ions in SrFFeAs, the structural phase transition is suppressed and the superconductivity occurs. $Sr_{1-x}La_xFFeAs$ and $Sr_{1-x}Sm_xFFeAs$ are reported to be superconductors with $T_c$ of 29K and 59 K, respectively. Then, we have firstly prepared $Sr_{1-x}Nd_xFFeAs$ and investigated their electric and magnetic properties. Moreover, even if a part of the Fe site is directly substituted by Co ions in the FeAs-layer, it is reported that superconductivity occurrs at 4 K. If the extra number of *d* electrons is important for the occurrence of superconductivity, Ni ions are considered to be more effective for the superconductivity. Then, we have prepared $SrFFe_{1-x}Ni_xAs$ and investigated their electric and magnetic properties. $Li_xFeAs$ itself is a superconductor with $T_c$ of 18 K. On the other hand, a homologous no superconducting compound $Na_xFeAs$ becomes to show a superconductivity when a part of the Fe site is substituted by Co and Ni ions. Then, we have prepared $Li_xFe_{1-y}Co_yAs$ and investigated their electric and magnetic properties.

## 2. Experimental Results and Discussions

### 2.1 Superconductivity in $Sr_{1-x}Nd_xFFeAs$

Almost single phase samples of $Sr_{1-x}Nd_xFFeAs$ are prepared for $0 \leq x \leq 0.5$ although tiny amounts of $SrF_2$ and $FeAs_2$ are observed. Lattice constants *a* and *c* decrease and $T_c$ increases with increasing *x*. The highest $T_c$ is 49 K for $Sr_{0.5}Nd_{0.5}FFeAs$. This value is comparable with that of $Sr_{1-x}Sm_xFFeAs$. The value of the temperature derivative of the upper critical magnetic field ($dH_{c2}/dT$) at $T_c$ is -1.5 T/K and the estimated value of $H_{c2}$ at 0 K becomes 75 T, assuming the parabolic approximation.

### 2.2 Electrical Properties of $SrFFe_{1-x}Ni_xAs$

Almost single phase samples of $SrFFe_{1-x}Ni_xAs$ are prepared for $0 \leq x \leq 0.2$ although a tiny amount of $SrF_2$ is observed. Lattice constants *a* and *c* decrease with increasing *x*. The kink temperature observed in the $\rho$-*T* curve which is due to the structural phase transition decreases with increasing *x*. Although all samples show a metallic conductivity, they are not superconducting above 3K.

### 2.3 Electrical and Magnetic Properties of $Li_xFe_{1-y}Co_yAs$

The Li content *x* is not precisely determined. Almost single phase samples of $Li_xFe_{1-y}Co_yAs$ are prepared for $0 \leq y \leq 0.05$ although a tiny amount of $Co_5As_2$ is observed. Lattice constants *a* and *c* and $T_c$ decrease with increasing *x*. The values of $T_c$, $dH_{c2}/dT$ at $T_c$, the lower critical magnetic field and the superconducting volume fraction of $Li_xFeAs$ and $Li_xFe_{0.98}Co_{0.02}As$ are 18K, -0.43 K/T, 0.05T and 54 %, and 11K, -0.43 K/T, 0.02T and 46 %, respectively. Although $Li_xFe_{0.95}Co_{0.05}As$ shows a drastic decrease in the electrical resistivity at 11 K, it does not show a zero resistive state.

## 3. Conclusion

We have explored the new high $T_c$ layered Fe-based superconductors and related compounds, and investigated the electrical and magnetic properties of them. However, the fabrication of superconducting thin films is necessary for the electronics use. We have collaborated in the research on $(Sr_{1-x}La_xF)FeAs$ thin films with professor K. Suzuki. A part of this collaboration was presented at the international conference of thin films in this year.

# Ultra Fast Information Recording and Ultra Fast Photo Magnetic Switching

**Arata TSUKAMOTO, Akiyoshi ITOH**
Information Storage; Supramolecules and Self-Assembly

## 1. Resarch aim

The ever increasing the capacity of storing information motivates the search for faster approaches to process and magnetically record information. Most computers store data on magnetic hard disk drives, in which the direction – "up" or "down" – of the magnetic moments in a small region of the disk corresponds to a binary bit. However, it was faced to unavoidable fundamental problem for faster operation in conventional way. We have experimentally demonstrated controlled magnetization reversal induced by a single 40 femtosecond ($40 \times 10^{-15}$s) circularly polarized laser pulse in the magnetic GdFeCo thin film, a material relevant for data storage. No external magnetic field is required for this photo-magnetic switching, and the stable final state of the magnetization is unambiguously determined by the helicity of the laser pulse. This finding, previously believed to be fundamentally impossible, reveals an ultrafast and efficient pathway for writing magnetic bits at 100000 times faster speeds compared with the conventional Hard Disk Drive. Based on these new discoveries, we are striving to establish the fundamental techniques of researching and developing ultrafast spin manipulation.

## 2. Research plan /Advances and achievements in 2010

We focused onto following concrete plans.

1) Preparation to measure the magnetic and optical response of material within sub-picosecond time resolution by femto-second laser pulse
2) Excitation of laser induced magnetization reversal phenomena in TbFeCo thin film

<Advances and achievements>

1) All-optical time resolved measurement system was constructed with femto-second pulse laser. Magnetic and optical response from material was monitored by the magneto optical effect and the change of reflectivity caused by heating of electrons, respectively. Ultrafast demagnetization phenomena were observed which must caused by heating of electron system. Here, time resolved study of magnetization response excited by 800 nm light and probed by 420 nm light shows both Gd and FeCo sublattice magnetizations are considerably reduced on the subpicosecond time scale. Fig. 1 shows the demonstration of thermo-magnetic recording by ultra-short single laser pulse (FWHM: 90 fs). The magnetization that laser irradiated area reversed by stray field created by surrounding magnetization.

2) We demonstrate that via careful tuning of the conditions in circularly polarized laser irradiation, it is possible that non-thermal effect overcome the usually dominating heat-driven effects of light on the magnetization in the metallic ferrimagnet GdFeCo. Fig. 2 shows the demonstrated result of photo magnetic switching of magnetization by circularly polarized light. Furthermore, Perpendicular magnetized TbFeCo thin film consisted from rare earth and transition metal alloy was prepared. We clarified that the magnetization direction of TbFeCo can be switched by irradiation of circularly polarized ultra short pulsed laser without magnetic field.

# Propagation Characteristics of Dielectric Waveguides with Arbitrary Inhomogeneous Media in the Middle Layer

**Tsuneki YAMASAKI**
Quantum Theory and Computation

In the working scheme at current year 2010, we analyzed the guiding problem of dielectric waveguide with arbitrary inhomogeneous media in the middle layer, and investigated the complex propagation constants by using the combination of improved Fourier series expansion method and multilayer method.

Numerical results are given by complex propagation constants in the stop band region for the case of various triangular pillar for both $TE_0$ and $TM_0$ modes as follows:

(1) The Stop-band area moves to the low frequency number side in the permittivity because an equivalent permittivity grows when changing. It begins to be different of the permittivity distribution by the frequency in the upper part of the Stop-band area.

(2) In $TE_0$mode, the influence of the characteristic doesn't appear when the circular cylinder is equal to an equivalent permittivity of the triangular pillar.

(3) In $TM_0$mode, the difference of shape influences the characteristic, and the Stop-band area broadens.

References

(1) R. Ozaki, T. Yamasaki, and T. Hinata: “Propagation Characteristics of Dielectric Waveguide with arbitrary inhomogeneous media in the middle layer”, IEEJ Technical Report EMT-10-163( 2010).